A Compact Waveguide "Resolver" for the Accurate Measurement of Complex Reflection and Transmission Coefficients Using the 6-Port Measurement Concept

GORDON P. RIBLET, MEMBER, IEEE

Abstract—**The theory of an optimum 5-port network for measuring complex reflection and transmission coefficients is developed. A compact realization in waveguide is described which allows these quantities to be determined over waveguide bandwidths from the measurement of two referenced power levels.**

I. Introduction

Recently, Engen has developed the theory for an optimum 6-port network for measuring complex reflection coefficients and has suggested several practical realizations [1], [2]. In many cases a 5-port would be sufficient, however. This is particularly the case if one is interested in measuring relatively small reflection coefficients such as those corresponding to a VSWR $<2/1$. In this paper the theory of the optimum 5-port is developed. A compact realization in waveguide operating over waveguide bandwidths is described and experimental data provided at *X*-band (8.2–12.4 GHz) and *Ku*-band (12.4–18.0 GHz). By including a precision rotary vane attenuator at the output, it is possible to overcome the restriction to small VSWR's and make accurate measurements of Γ's of any magnitude. Furthermore, by including the unit in a phase bridge it is possible to measure transmission coefficients in addition to reflection coefficients.

II. Theory of the Optimum 5-Port

Engen has introduced a diagram in the complex Γ plane which is quite useful for determining the circumstances under which Γ can be unambiguously and accurately determined from the measurement of the power levels at a number of detectors [2]. One of these detectors is connected to a directional coupler and serves to monitor the incident power. Each additional detector can be represented by a point q_i in the Γ plane. Engen has suggested that the optimum situation in terms of accuracy arises when there are three additional detectors and the points q_i are separated by 120° on a circle with its center at the origin and diameter >1. The device will have a total of 6 ports when the signal port and a port for the device under test are included. He has, however, pointed out that in principle 5-ports are sufficient. We will be considering here a 5-port version of the 6-port scheme (see Fig. 1 for a schematic diagram).

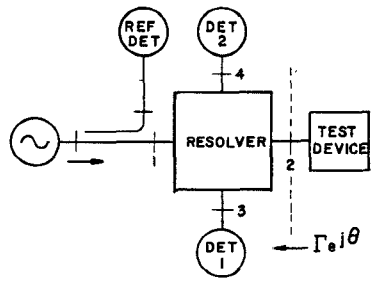

Fig. 1. Schematic diagram of an experimental arrangement for the measurement of Γ with a 5-port.

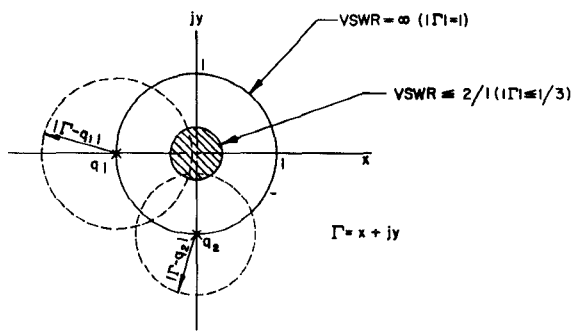

Fig. 2. Optimum location of the points q_1, q_2 in complex Γ plane for the measurement of small VSWR's with a 5-port.

It will be argued that for small VSWR's ($\rho<2/1$) the optimum 5-port network has two additional detectors with q values q_1 and q_2 separated by 90° on the unit circle. In this case Γ will be uniquely determined by the intersection of 2 circles of known radius as indicated in Fig. 2. The intersection outside of the unit circle can be discarded. Since the circles intersect at nearly 90° independent of phase within the hatched area, the accuracy will be nearly independent of the actual reflected phase θ.

Manuscript received July 28, 1980; revised September 15, 1980.

The author is with Microwave Development Laboratories, Inc., Natick, MA 01760.

0018-9480/81/0200-0155$00.75 ©1981 IEEE

If $|A|$ is the amplitude of the incident signal then

$$P_{REF} = |C_{REF}|^2 |A|^2 \tag{1}$$

$$P_1 = |C_1|^2 |A|^2 |\Gamma - q_1|^2 \tag{2}$$

$$P_2 = |C_2|^2 |A|^2 |\Gamma - q_2|^2 \tag{3}$$

where P_{REF}, P_1, P_2 are the powers measured at the reference detector, detector 1, and detector 2, respectively, while $|C_{REF}|^2, |C_1|^2, |C_2|^2$ are coupling factors. Without loss of generality we may say that $|C_{REF}|^2 = |C_1|^2 = |C_2|^2$ since any difference in these factors can be referenced out in a computer or microprocessor based measurement system by taking a reference reading with a load on the output. Nevertheless it is desireable in practice to have the terms approximately equal. In this case it follows from (1), (2), and (3) that

$$P_1/P_{REF} = |\Gamma + 1|^2 = 1 + |\Gamma|^2 + 2|\Gamma| \cos\theta \tag{4}$$

$$P_2/P_{REF} = |\Gamma + j|^2 = 1 + |\Gamma|^2 + 2|\Gamma| \sin\theta \tag{5}$$

assuming that $q_1 = -1$, $q_2 = -j$. Equations (4) and (5) are the basic "resolver" equations for determining $|\Gamma|$ and θ in terms of measured power ratios P_1/P_{REF}, P_2/P_{REF}. If we denote these ratios simply as $\bar{P}_1$ and $\bar{P}_2$, then the magnitude of Γ is given by the simple expression

$$|\Gamma|^2 = \frac{\bar{P}_1 + \bar{P}_2}{2} - \sqrt{\left(\frac{\bar{P}_1 + \bar{P}_2}{2}\right)^2 - \left(\frac{\bar{P}_1 - 1}{2}\right)^2 - \left(\frac{\bar{P}_2 - 1}{2}\right)^2}\,. \tag{6}$$

The fact that the measurement accuracy is independent of phase angle for small reflection coefficients can be demonstrated quite clearly by taking the logarithm of both sides of (4) and (5) and considering the limit $|\Gamma| \ll 1$. In this case

$$\log_e \bar{P}_1 \simeq \log_e(1 + 2|\Gamma| \cos\theta) \simeq 2|\Gamma| \cos\theta$$

$$\log_e \bar{P}_1 \simeq \log_e(1 + 2|\Gamma| \sin\theta) \simeq 2|\Gamma| \sin\theta.$$

Consequently, with a dual channel scope with logarithmic outputs and the memory subtraction feature (such as PMI's Model #1038) the two outputs will be directly proportional to the Smith chart variables in the limit of small $|\Gamma|$! This can be demonstrated by: 1) connecting the reference detector to the reference channel, detector 1 to channel A, detector 2 to channel B; 2) storing a reference measurement with a good load in the memory of both channels; 3) plotting the 2 outputs from the scope on an x–y recorder with the unit to be tested on the line.

III. A Waveguide Realization

So far values have been found for q_1 and q_2 which allow for the unambiguous determination of Γ for the case of small VSWR's—which is the case of the most practical interest. However, this still doesn't tell us how to construct a circuit to yield such values. To see how to do this it is best to express P_1 and P_2 in terms of the S matrix elements of the network of Fig. 1. Assuming $S_{22} = 0$ and well matched detectors

$$P_1 = \{S_{13} + S_{23}S_{12}\Gamma\}\{S_{13}^* + S_{23}^* S_{12}^* \Gamma^*\}$$

$$P_2 = \{S_{14} + S_{24}S_{12}\Gamma\}\{S_{14}^* + S_{24}^* S_{12}^* \Gamma^*\}.$$

Therefore

$$P_1 = |S_{13}|^2 + |S_{23}|^2 |S_{12}\Gamma|^2 + (S_{13}S_{23}^* S_{12}^* \Gamma^* + S_{13}^* S_{23} S_{12}\Gamma) \tag{7}$$

$$P_2 = |S_{14}|^2 + |S_{24}|^2 |S_{12}\Gamma|^2 + (S_{14}S_{24}^* S_{12}^* \Gamma^* + S_{14}^* S_{24} S_{12}\Gamma). \tag{8}$$

Comparison with (1)–(5) indicates that the conditions on the S-matrix entries are

$$S_{13} = S_{23} \tag{9}$$

$$S_{14} = e^{j\pi/2} S_{24} \tag{10}$$

$$S_{12} = 1. \tag{11}$$

A further condition which in practice need not hold exactly is $|S_{13}| = |S_{14}|$. Using the reciprocity principle one sees that condition (9) requires that the signal divide equally out of ports 1 and 2 when feeding port 3 and that condition (10) requires that the signals from these ports should differ only in a phase shift of 90° when feeding port 4. The general S matrix of the basic four port network has the form then

$$S = \begin{bmatrix} 0 & S_{12} & S_{13} & S_{14} \\ S_{12} & 0 & S_{13} & S_{14}e^{j\pi/2} \\ S_{13} & S_{13} & X & Y \\ S_{14} & S_{14}e^{j\pi/2} & Y & Z \end{bmatrix}$$

where $|S_{12}| \lesssim 1$ and X, Y, Z can be anything. If the network were lossless, then unitarity would require that the dot product of the first column of S with the complex conjugate of the second column of S be 0, i.e.,

$$|S_{13}|^2 + |S_{14}|^2 e^{-j\pi/2} = 0.$$

Since this is clearly impossible, the ideal network must contain lossy elements.

Condition (11) is impossible to satisfy exactly. However, the approximate condition $|S_{12}| \simeq 1$ is easily satisfied by making the coupling to detectors 1 and 2 weak (30 dB or so). In that case (4) and (5) will apply to a high degree of accuracy if one remembers that θ also includes the phase shift due to S_{12}. This phase term can be removed by an appropriate shift of the reference plane. The weak coupling condition which can be stated as

$$|S_{12}| \lesssim 1 \tag{12}$$

has some practical advantages. For a typical input power of +10 dBm and 30 dB coupling, the power to the detectors will be −20 dBm. This is large enough that the signal won't be noisy but not so large as to be in the highly nonlinear region of most crystal detectors. Furthermore, because of the weak coupling, the errors introduced by detector mismatches and imperfect components will be minimized.

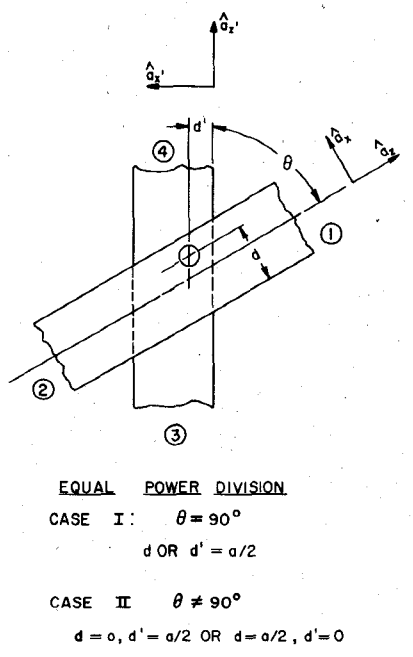

Fig. 3. The coupling between two waveguides through a single hole in the top wall of the type considered in the text.

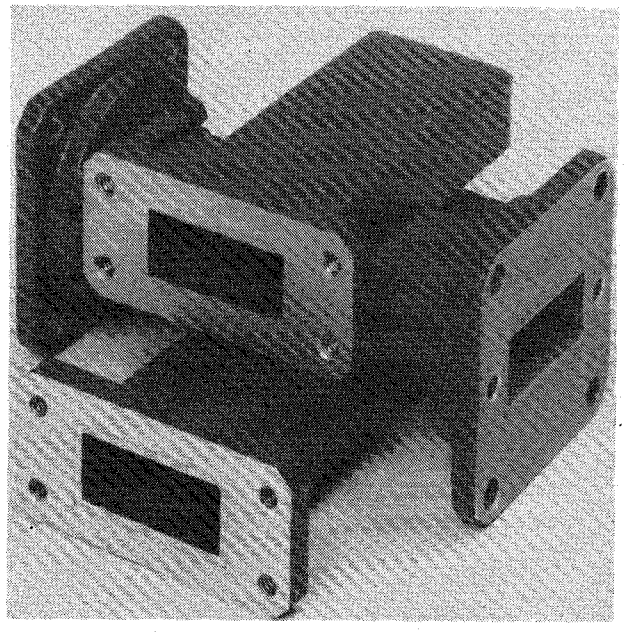

Fig. 4. The picture of a WR90 waveguide resolver.

In waveguide one of the simpler possible ways for satisfying condition (9) or (10) is by coupling the main arm to a secondary arm through an appropriately positioned hole as in Fig. 3. This is particularly so since 30-dB coupling is readily obtainable with a single coupling hole. The secondary arm for detector 1 could be located on the top wall of the main arm while the secondary arm for detector 2 could be located on the bottom wall. The coupling holes for these detectors should be located at the same main arm reference plane. The unused secondary arm ports are terminated in loads. These are the lossy elements referred to above. Note that reflections from these loads or from the detectors only effect the coupling levels and not the power division properties of the device. Any coupling variations are removed when a reference measurement is taken with a sliding load on the output. The resulting structure, which resembles a "double" cross guide coupler, is shown in Fig. 4.

A condition common to (9) and (10) is that the power divide equally out of ports 1 and 2 when feeding the detector port. There should be no directivity. Using the Bethe small hole coupling theory [3], we can attempt to find out under what circumstances this condition will be satisfied independent (hopefully!) of frequency. In fact one can show (see Appendix) that there are two situations which lead to equal power division independent of frequency.

Case I:

$$\theta = 90°(\cos\theta = 0);\ d \text{ or } d' = a/2 \text{ (refer to Fig. 3)}$$

i.e., the waveguides are at right angles and the hole is centered in one of the waveguides.

Case II:

$$\theta \neq 90°;\ d = 0,\ d' = a/2 \text{ or } d = a/2,\ d' = 0$$

i.e., the waveguides are not at right angles but the hole is centered in one waveguide and against the wall of the other. The angle θ is that between the two waveguide arms.

It is not possible to satisfy (10) using Case II so that this case won't be considered further. Condition (9) is easy to satisfy using Case I. One simply lets the hole be centered in the secondary arm (off center in the main arm). From symmetry and reciprocity it follows that $S_{13} = S_{31} = S_{32} = S_{23}$. Condition (10) is more difficult to satisfy. The hole will clearly have to be off center in the secondary arm and centered in the main arm. Within a common proportionality factor the S matrix elements S_{14}, S_{24} are given by the Bethe theory as

$$S_{14} = -\alpha_e \frac{\lambda_g^2}{\lambda^2} \sin\frac{\pi d}{a} + j\frac{\lambda_g}{a}\alpha_m(1)\cos\frac{\pi d}{a} \tag{13}$$

$$S_{24} = -\alpha_e \frac{\lambda_g^2}{\lambda^2} \sin\frac{\pi d}{a} - j\frac{\lambda_g}{a}\alpha_m(1)\cos\frac{\pi d}{a} \tag{14}$$

where λ_g is the guide wavelength, λ is the wavelength, a is the guide width, d is the distance of the center of the hole from the waveguide wall in the secondary arm, α_e and $\alpha_m(1)$ are electric and magnetic polarizabilities of the hole. It is apparent from (13) and (14) that the phase θ of S_{24} with respect to S_{14} may be varied by varying the distance d of the hole from the wall of the secondary arm. The phase difference is given by

$$\theta = 2\tan^{-1}\frac{\lambda^2}{a\lambda_g}\frac{\alpha_m(1)}{\alpha_e}\cot\frac{\pi d}{a}$$

$$= 2\tan^{-1}\sqrt{\lambda^2 - \lambda^4/\lambda_c^2}\,\frac{\alpha_m(1)}{a\alpha_e}\cot\frac{\pi d}{a} \tag{15}$$

where λ_c is the cutoff wavelength of the waveguide. In

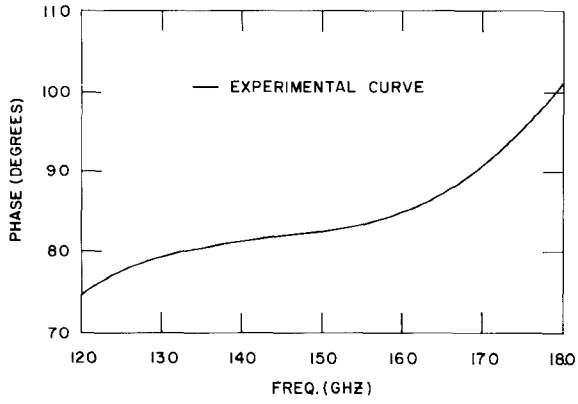

Fig. 5. The experimental phase difference between signals from the main line ports when feeding the lower secondary arm port of a WR62 resolver. This difference should ideally be 90°.

what follows it will be assumed that circular holes for which $\alpha_m(1)=\alpha_e$ are being used. These holes give the largest coupling for a given value of θ. If $\theta=90°$ as well then

$$d=\frac{a}{\pi}\tan^{-1}\frac{\lambda^2}{a\lambda_g}. \tag{16}$$

This formula determines the required hole location in terms of a and λ. For WR90 waveguide at 9.375 GHz, $d=0.225$ in. Ideally the phase difference θ should be 90° independent of frequency. Clearly from (15), this won't be the case in practice. However, it will track 90° fairly closely over a waveguide band. It can readily be shown that $d\theta/d\lambda=0$ for some frequency within the waveguide band. It follows from (15) that $d\theta/d\lambda=0$ if $d(\lambda^2-\lambda^4/\lambda_c^2)/d\lambda=0$. Now

$$\frac{d(\lambda^2-\lambda^4/\lambda_c^2)}{d\lambda}=2\lambda-4\lambda^3/\lambda_c^2=0\Rightarrow\lambda=\lambda_c/\sqrt{2}\,.$$

For WR90 waveguide this will occur at 9.273 GHz. One might expect the variation in θ to be small over the waveguide band 8.2–12.4 GHz. In practice it is significant and must be corrected for in the computer program which evaluates the measurement data [4].

Fig. 4 gives the picture of an actual WR90 waveguide resolver constructed according to the principles outlined above. A hole 0.312 in in diameter with a wall thickness of 0.030 in gave a coupling of 30 dB ± 1.5 dB from 8.2–12.4 GHz. An input VSWR < 1.07 and coupling unbalance < 0.2 dB (for both secondary arms) from 8.2 to 12.4 GHz was achieved.

Any small deviations from ideal performance aren't serious however because, as is usual in 6-port work, the actual calibration constants of the resolver can be employed to calculate Γ. In particular the actual S matrix entries can be employed in (7) and (8). $\bar{P}_1$ and $\bar{P}_2$ will in any case be linear in $|\Gamma|^2$, $|\Gamma|\cos\theta$, and $|\Gamma|\sin\theta$. It is then always possible to arrive at an equation quadratic in $|\Gamma|^2$ which will have a solution similar in form to that of (6). This assumes that the directional coupler used to monitor the incident power has infinite directivity. Since commercial waveguide couplers with directivities >40 dB over a waveguide band are readily available, this is a good approximation. Because the detectors are decoupled from one another by 60 dB, the calibration is determined by the mechanical structure of the 4-port device given in Fig. 4 for all practical purposes.

The major deviation from ideal performance has been found to occur for the phase difference θ, which ideally should be 90° over a waveguide band. It was pointed out that according to the Bethe theory, the angle θ should have a maximum within the waveguide band. This would suggest that the deviation from 90° over a waveguide band could be expected to be small. Experimentally, it has been found that the frequency dependence of θ follows more nearly an S shaped curve at a coupling level of about 30 dB. The results for a *Ku*-band unit are summarized in Fig. 5. The solid curve is determined from experimental points. The accurate treatment of the coupling through such holes would require the inclusion of the effect of wall thickness. Such treatments have up until now been only partly successful.

IV. Some Experimental Determinations of Reflection and Transmission Coefficients at *Ku*-Band (WR62)

Recently, measurements of VSWR and transmission phase using *X*-band (WR90) and *Ku*-band (WR62) resolvers have been reported [4],[5]. In this section more results will be presented at *Ku*-band. The reflection coefficient Γ can be measured by simply connecting the device under test (DUT) at the output. A transmission coefficient Υ can be measured by incorporating the resolver into a phase bridge [5]. The phase bridge arrangement has the advantage that, with minor modifications, it allows both Γ and Υ to be measured. The schematic diagram of a *Ku*-band bridge arrangement is given in Fig. 6. Power from a signal generator divides along the two branches of the bridge. If one wants to measure the reflection coefficient alone, then the power along branch 2 is terminated in a load, isolator 2 is removed and the DUT is connected directly to the output of the precision rotary vane attenuator. The diagram indicates that a PMI 1045 power meter is used as the basic power detection unit. Most of our measurement have in fact used the PMI 1038 scope, however. The detector associated with the reference cou-

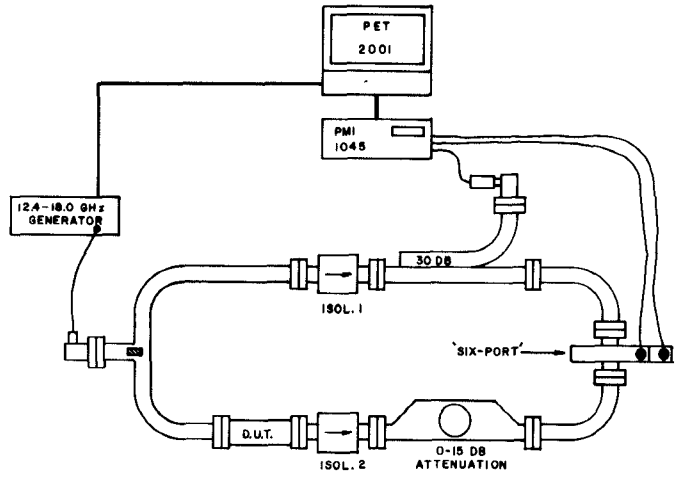

WR 62 (12.4-18.0 GHz)
TRANSMISSION PHASE MEASUREMENT SYSTEM

Fig. 6. WR62 (12.4–18.0 GHz) transmission phase measurement system.

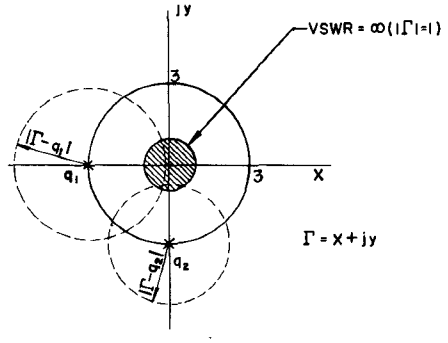

Fig. 7. The location of the points q_1, q_2 in the complex Γ plane with a precision rotary vane attenuator with 4.77 dB of attenuation inserted in front of resolver.

TABLE I
MEASUREMENT OF SOME STANDARDS WITH A WR62 WAVEGUIDE RESOLVER

Freq. (MHz)	1.05 VSWR	1.10 VSWR	1.20 VSWR	1.50 VSWR	RE-REF.
12400	1.049	1.101	1.202	1.508	1.001
13100	1.050	1.103	1.196	1.512	1
13800	1.049	1.101	1.199	1.509	1.001
14500	1.049	1.103	1.204	1.521	1.001
15200	1.047	1.099	1.196	1.508	1.002
15900	1.050	1.101	1.195	1.482	1.001
17300	1.051	1.102	1.212	1.524	1.002
18000	1.050	1.102	1.202	1.511	1 002

pler is connected to the reference channel while those associated with the resolver are connected to channels A and B. The unit is operated in the A/Ref, B/Ref mode on the 1-dB/cm scale.

Table I gives the results of some VSWR standard measurements using the bridge in the mode for measuring reflection coefficients described above. A reference was taken with a sliding load on the output of the precision rotary vane attenuator. With an attenuation setting appropriate to some VSWR standard (1.05, 1.10, 1.15, 1.20, 1.50) a measurement was made with a short circuit on the output of the attenuator. The measurement data were then evaluated using a computer program which compensated for the fact that the angle θ is not 90° over a waveguide band [4]. The results are summarized in the Table. The repeatability of a VSWR measurement can be 1.002 or less.

As has been pointed out previously, the 5-port will only allow accurate and unambiguous measurements of Γ to be made if the corresponding VSWR is less than 2/1. To be able to unambiguously measure Γ's of all magnitudes, we would have to use a genuine 6-port. However as a practical matter this restriction to small Γ's can readily be overcome by including a precision rotary vane attenuator at the output. This is illustrated in Fig. 7. By inserting 4.77 dB of attenuation, the q points q_1 and q_2 are in effect moved outward from -1, $-j$ to -3 and $-3j$. Furthermore, the hatched area corresponding to a VSWR $<2/1$ is now transformed into the entire unit circle. Γ can now be determined accurately within the entire unit circle with admittedly reduced repeatability for small VSWR measurements.

The phase bridge of Fig. 6 can be used to measure transmission coefficients Υ in a way very much analogous to the measurement of reflection coefficients. Its use to measure transmission phase has been described recently [5]. The measurement of Υ is possible because of the presence of isolator 2 between the device under test (DUT) and the precision rotary vane attenuator. This isolator removes the influence of the output reflection coefficient of the DUT. As with the measurement of Γ, an initial reference measurement must be made with a load on the output of isolator 2. If $|\Upsilon| > 1/3$, then attenuation must be introduced to allow unambiguous measurements to be made as explained previously. Suppose we wished to measure the transmission phase of a low-loss device such as an isolator or phase shifter. Then it is desirable to introduce 15 dB of attenuation through the rotary vane attenuator. Considering that commercial isolators with greater than 25-dB return loss over a waveguide band are

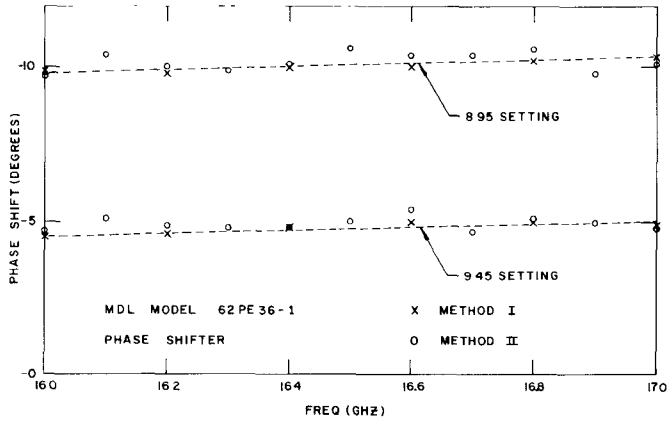

(a)

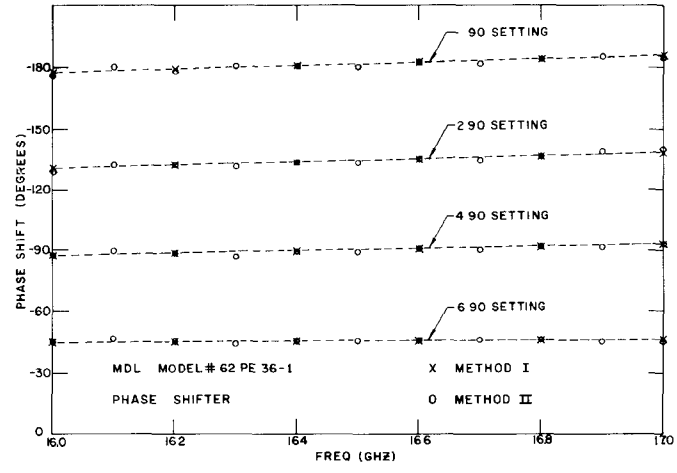

(b)

Fig. 8. The measurement of the phase shift introduced by a commercial *Ku*-band phase shifter for various settings.

readily available, the signal reflected off the output of isolator 1 will be 40 dB or more down from the main line signal and should introduce only a very small error.

In Fig. 8(a),(b) the results of some measurements of the relative transmission phase introduced by a narrow-band WR62 phase shifter (16.0–17.0 GHz) are given for various phase shifter settings. Fig. 8(a) gives the phase shift versus frequency for two settings which introduce relatively small phase shifts of 5 and 10 degrees, respectively. The results for the method just described are given by crosses. The results given by circles are for a second independent measurement technique described in [5] and confirm the correctness of the readings. The measurements are correct within 0.5° for small phase differences. Clearly the method is a quite accurate way to measure small phase differences —one of the more common applications. Fig. 8(b) gives results for settings which introduce approximately 45°, 90°, 135°, and 180° of phase shift. The accuracy decreases for larger phase differences but the disagreement is in no case greater than 3°.

IV. Conclusions

In this paper the theory of an optimum 5-port for measuring complex reflection coefficients has been developed. A practical waveguide realization was described and working models have been built in WR90 and WR62 waveguide. It was shown how the limitation to the measurement of small reflection coefficients can be overcome and how they can be used to measure transmission properties as well. Considerable experimental experience has been accumulated with these devices which confirms their usefulness.

Appendix

The class of waveguide structures we will be considering in an attempt to obtain relations similar to those of (4) and (5) will consist of two top wall coupled waveguides turned at an angle of θ degrees with respect to one another as in Fig. 3. The distance of the hole from the edge of the lower waveguide will be d', and from the upper waveguide it will be d. In this general case the S matrix elements S_{31}, S_{32} for electric dipole radiation are

$$S_{31} = S_{32} = -\alpha_e \frac{\lambda_g^2}{\lambda^2} \sin\frac{\pi d}{a} \cdot \sin\frac{\pi d'}{a} \qquad \text{(electric dipole)}$$

where α_e is proportional to the polarizability of the hole for electric dipole radiation [3]. Similarly, for magnetic dipole radiation

$$S_{31} = 2\left(\sin\frac{\pi d}{a}\hat{a}_x + j\frac{\pi}{\beta a}\cos\frac{\pi d}{a}\hat{a}_z\right) \cdot \left(\alpha_m(1)\sin\frac{\pi d'}{a}\hat{a}_x - j\alpha_m(2)\frac{\pi}{\beta a}\cos\frac{\pi d'}{a}a_{z'}\right)$$

$$S_{32} = 2\left(-\sin\frac{\pi d}{a}\hat{a}_x + j\frac{\pi}{\beta a}\cos\frac{\pi d}{a}\hat{a}_z\right) \cdot \left(\alpha_m(1)\sin\frac{\pi d'}{a}\hat{a}_x - j\alpha_m(2)\frac{\pi}{\beta a}\cos\frac{\pi d'}{a}\hat{a}_{z'}\right)$$

where $\alpha_m(1)$, $\alpha_m(2)$ are proportional to the two polarizability components for magnetic dipole radiation while $\hat{a}_x$, $\hat{a}_z$, and $\hat{a}_{x'}$, $\hat{a}_{z'}$ are unit vectors directed across and along the upper and lower guides, respectively. Since θ is the angle between the waveguides, $\hat{a}_x \cdot \hat{a}_{x'} = \hat{a}_z \cdot \hat{a}_{z'} = \cos\theta$ while $\hat{a}_x \cdot \hat{a}_{z'} = -\sin\theta$ and $\hat{a}_{x'} \cdot \hat{a}_z = \sin\theta$. Therefore

$$S_{31} = 2\cos\theta\left\{\alpha_m(1)\sin\frac{\pi d}{a}\sin\frac{\pi d'}{a} + \frac{\pi^2}{\beta^2 a^2}\alpha_m(2)\cos\frac{\pi d}{a}\cos\frac{\pi d'}{a}\right\} + \frac{2\pi j}{\beta a}\sin\theta\left\{\alpha_m(1)\cos\frac{\pi d}{a}\sin\frac{\pi d'}{a} + \alpha_m(2)\sin\frac{\pi d}{a}\cos\frac{\pi d'}{a}\right\}$$

$$S_{32} = 2\cos\theta\left\{-\alpha_m(1)\sin\frac{\pi d}{a}\sin\frac{\pi d'}{a} + \frac{\pi^2}{\beta^2 a^2}\alpha_m(2)\cos\frac{\pi d}{a}\cos\frac{\pi d'}{a}\right\} + \frac{2\pi j}{\beta a}\sin\theta\left\{\alpha_m(1)\cos\frac{\pi d}{a}\sin\frac{\pi d'}{a} - \alpha(2)\sin\frac{\pi d}{a}\cos\frac{\pi d'}{a}\right\}$$

for magnetic dipole radiation. The total amplitudes propagated to ports 1 and 2, respectively, are given by adding the contributions of the electric and magnetic dipoles. These are

$$S_{31}^T = \left(2\alpha_m(1)\cos\theta - \alpha_e\frac{\lambda_g^2}{\lambda^2}\right)\sin\frac{\pi d}{a}\sin\frac{\pi d'}{a} + \frac{2\pi^2}{\beta^2 a^2}\alpha_m(2)\cos\theta\cos\frac{\pi d}{a}\cos\frac{\pi d'}{a} + \frac{2\pi j}{\beta a}\sin\theta\left\{\alpha_m(1)\cos\frac{\pi d}{a}\sin\frac{\pi d'}{a} + \alpha_m(2)\sin\frac{\pi d}{a}\cos\frac{\pi d'}{a}\right\}$$

$$S_{32}^T = \left(-2\alpha_m(1)\cos\theta - \alpha_e\frac{\lambda_g^2}{\lambda^2}\right)\sin\frac{\pi d}{a}\sin\frac{\pi d'}{a} + \frac{2\pi^2}{\beta^2 a^2}\alpha_m(2)\cos\theta\cos\frac{\pi d}{a}\cos\frac{\pi d'}{a} + j\frac{2\pi}{\beta a}\sin\theta\left\{\alpha_m(1)\cos\frac{\pi d}{a}\sin\frac{\pi d'}{a} - \alpha_m(2)\sin\frac{\pi d}{a}\cos\frac{\pi d'}{a}\right\}.$$

Under what conditions can equal power division be achieved independent of frequency? Upon evaluating $S_{31}^T S_{31}^{T*} - S_{32}^T \cdot S_{32}^{T*}$ and canceling common terms one finds that this condition becomes

$$-8\alpha_m(1)\alpha_e\frac{\lambda_g^2}{\lambda^2}\cos\theta\sin^2\frac{\pi d}{a}\sin^2\frac{\pi d'}{a} + \frac{16\pi^2}{\beta^2 a^2}\cdot\alpha_m(1)\alpha_m(2)\cos^2\theta\left\{\sin\frac{\pi d}{a}\sin\frac{\pi d'}{a}\cdot\cos\frac{\pi d}{a}\cos\frac{\pi d'}{a}\right\} + \frac{16\pi^2}{\beta^2 a^2}\alpha_m(1)\alpha_m(2)\sin^2\theta\cdot\left\{\sin\frac{\pi d}{a}\sin\frac{\pi d'}{a}\cos\frac{\pi d}{a}\cos\frac{\pi d'}{a}\right\} = 0$$

$$\Rightarrow \frac{2\pi^2}{\beta^2 a^2}\alpha_m(1)\alpha_m(2)\cos\frac{\pi d}{a}\cos\frac{\pi d'}{a} = \alpha_e\frac{\lambda_g^2}{\lambda^2}\cos\theta\sin\frac{\pi d}{a}\sin\frac{\pi d'}{a}.$$

This equation must be satisfied independent of frequency, i.e., both sides must be identically 0 since λ^2 is frequency dependent. There are several cases.

Case I:

$$\theta = 90°(\cos\theta = 0) \Rightarrow d \text{ or } d' = a/2.$$

If the waveguide arms are at right angles, then the hole must be centered in one of the waveguides.

Case II:

$$\theta \neq 90° \Rightarrow d = 0,\ d' = a/2 \text{ or } d = a/2,\ d' = 0.$$

If the arms are not at right angles, then the hole must be centered in one guide and against the wall in the other.

For case I

$$S_{31}^T = -\alpha_e\frac{\lambda_g^2}{\lambda^2}\sin\frac{\pi d'}{a} + j\frac{2\pi}{\beta a}\alpha_m(2)\cos\frac{\pi d'}{a} \qquad (d = a/2)$$

$$S_{32}^T = -\alpha_e\frac{\lambda_g^2}{\lambda^2}\sin\frac{\pi d'}{a} - j\frac{2\pi}{\beta a}\alpha_m(2)\cos\frac{\pi d'}{a} \qquad (d = a/2) \qquad \text{(A)}$$

or

$$S_{31}^T = -\alpha_e\frac{\lambda_g^2}{\lambda^2}\sin\frac{\pi d}{a} + j\frac{2\pi}{\beta a}\alpha_m(1)\cos\frac{\pi d}{a} \qquad (d' = a/2)$$

$$S_{32}^T = -\alpha_e\frac{\lambda_g^2}{\lambda^2}\sin\frac{\pi d}{a} + j\frac{2\pi}{\beta a}\alpha_m(1)\cos\frac{\pi d}{a} \qquad (d' = a/2). \qquad \text{(B)}$$

For case II

$$S_{31}^T = j\frac{2\pi}{\beta a}\alpha_m(1)\sin\theta \text{ or } j\frac{2\pi}{\beta a}\alpha_m(2)\sin\theta$$

$$S_{32}^T = j\frac{2\pi}{\beta a}\alpha_m(1)\sin\theta \text{ or } -\frac{2\pi}{\beta a}\alpha_m(2)\sin\theta.$$

The expressions (A) are of particular interest because the signals to ports 1 and 2 can be made to be out of phase by any amount by an appropriate choice of the distance d'. For the other cases they are either in phase or 180° out of phase independent of frequency. The equations (A) can be rewritten as

$$S_{31}^T = \sqrt{\alpha_e^2\frac{\lambda_g^4}{\lambda^4}\sin^2\frac{\pi d'}{a} + \frac{4\pi^2}{\beta^2 a^2}\alpha_m^2(2)\cos^2\frac{\pi d'}{a}}\; e^{-j\theta'/2 + j\pi}$$

$$S_{32}^T = \sqrt{\alpha_e^2\frac{\lambda_g^4}{\lambda^4}\sin^2\frac{\pi d'}{a} + \frac{4\pi^2}{\beta^2 a^2}\alpha_m^2(2)\cos^2\frac{\pi d'}{a}}\; e^{j\theta'/2 + j\pi}$$

where

$$\theta' = 2\tan^{-1}\frac{\lambda^2\alpha_m(2)}{a\lambda_g\alpha_e}\cot\frac{\pi d'}{a} = 2\tan^{-1}\frac{\sqrt{\lambda^2 - \lambda^4/\lambda_c^2}}{a}\frac{\alpha_m(2)}{\alpha_e}\cot\frac{\pi d'}{a}$$

where a is the guide width, λ_c is its cutoff wavelength, d' is the distance of the hole from the edge of the guide, $\alpha_e, \alpha_m(2)$ are its electric and magnetic polarizabilities, respectively. Clearly $d\theta'/d\lambda = 0$ if $d(\lambda^2 - \lambda^4/\lambda_c^2/d\lambda = 0$. Now

$$\frac{d(\lambda^2 - \lambda^4/\lambda_c^2)}{d\lambda} = 2\lambda - 4\lambda^3/\lambda_c^2 = 0$$

$$\Rightarrow \lambda = \lambda_c/\sqrt{2}.$$

In the case of WR90 waveguide this will occur at 9.273 GHz. One can consequently expect θ to vary only slightly over the 8.2–12.4-GHz band.

REFERENCES

[1] Glenn F. Egen, "An improved circuit for implementing the six-port technique of microwave measurements," *IEEE Trans. Microwave Theory Tech.*, vol. MTT-25, pp. 1080–1083, Dec. 1977.

[2] Glenn F. Engen, "The six-port reflectometer: An alternate network analyser," *IEEE Trans. Microwave Theory Tech.*, vol. MTT-25, pp. 1075–1080, Dec. 1977.

[3] R. E. Collin, *Foundations for Microwave Engineering*. New York: McGraw-Hill, 1966.

[4] G. P. Riblet, "A compact waveguide "resolver" for the accurate measurement of complex reflection coefficients using the six-port measurement concept," in *IEEE MTT-S 1979 Int. Microwave Symp. Dig.*, May 1979, pp. 60–62.

[5] G. P. Riblet, "Transmission phase measurements with a single six-port," *IEEE MTT-S 1980 Int. Microwave Symp. Dig.*, May 1980, pp. 431–433.

Short Papers

Suspended Coupled Slotline Using Double Layer Dielectric

RAINEE N. SIMONS, MEMBER, IEEE

Abstract—**This paper presents a rigorous analysis of coupled slotline a) on a double-layer dielectric substrate, and b) sandwiched between two dielectric substrates. The dielectric substrates are of arbitrary thickness and permittivity and the structure is assumed to be suspended inside a conducting enclosure of arbitrary dimensions. The odd- and even-mode dispersion and characteristics impedance, along with the effect of shielding on these, are illustrated. These structures should find extensive applications in the fabrication of MIC components, such as directional couplers, phase shifters, and mixers.**

I. INTRODUCTION

Slotline on a dielectric substrate [1] is ideally suited for MIC components, such as directional couplers [2], phase shifters [3], and balanced mixers [4]. Alumina, which is the usual choice of the substrate material at X-band and below, is excessively dispersive at millimeter-wave frequencies. By reducing the substrate thickness dispersion is reduced, but this results in extremely narrow linewidth which increases line loss and makes reproduction difficult [5]. Recently, two new slotline structures have been proposed; namely, slotline on a double-layer dielectric substrate [6] and the sandwich slotline [7]. The disadvantages inherent in the conventional slotline are overcome in the double-layer slotline where an additional dielectric layer of low permittivity is introduced between the ground plane containing the slot and the bottom dielectric layer. The sandwich slotline, with top dielectric layer of low permittivity, is also useful at millimeter-wave frequencies. However, it has a slightly higher value of effective dielectric constant when compared with the double-layer slotline with same permittivities.

The paper analyzes firstly, the coupled slotline on a double-layer dielectric substrate suspended inside a conducting enclosure of arbitrary dimensions, and, secondly, the coupled slotline sandwiched between two dielectric substrates suspended inside a conducting enclosure of arbitrary dimension. For the sake of convenience the dielectric substrates are of arbitrary thickness and permittivity. Invariably a practical system is shielded from the environment in order to protect it from RF interference. Hence the study also illustrates the effect of shielding on the computed odd- and even-mode dispersion and characteristic impedance.

Manuscript received June 5, 1980; revised September 11, 1980.

The author is with the Centre for Applied Research in Electronics, Indian Institute of Technology Delhi, Hauz Khas, New Delhi 110016, India.

II. ANALYSIS

A schematic diagram of the structures to be analyzed is shown in Fig. 1(a) and (b). For the case of odd excitation, a magnetic wall is placed at the $y=0$ plane (Fig. 1(c)); it then suffices to restrict the analysis to the right half of the structure. A similar simplification is possible for the case of even excitation except that the magnetic wall at the $y=0$ plane is replaced by an electric wall. Modifying Cohn's analysis of a slotline on a dielectric substrate [1], the odd- and even-mode structures can be easily reduced to an asymetric capacative iris backed by a double-layer dielectric substrate or sandwiched between two dielectric substrates in a rectangular waveguide (Fig. 1(d)). It then follows that for the odd excitation, the full set of modes satisfying the boundary conditions are the $TE_{1,n}$ and $TM_{1,n}(n \geqslant 0)$, and for the even excitation, $TE_{1,n}(n \geqslant 0)$ and $TM_{1,n}(n>0)$. The resulting expressions are given below for the odd mode only.

Let $p=\lambda/2a$ be an independent variable, where λ is the free-space wavelength and a is the length of the slot as in Cohn's analysis [1]. At the transverse resonance frequency $a=\lambda'/2$ and $p=\lambda/\lambda'$ for $B_t=0$, where λ' is the wavelength in the slotline and B_t is the total susceptance at the plane of the slot. Slotline on a double-layer dielectric (odd mode):

The total E_y and H_x fields at the $z=0$ plane and $x=a/2$ are functions of y as follows:

$$E_y = \sum_{n=0,1,2,\cdots}^{\infty} R_n \sin((2n+1)/2)\pi y/b \tag{1}$$

$$H_x = -\sum_{n=0,1,2,\cdots}^{\infty} y_{in} R_n \sin((2n+1)/2)\pi y/b. \tag{2}$$

Where the input wave admittance y_{in} is defined as in [1] and the

0018-9480/81/0200-0162$00.75